

Enhanced up-conversion luminescence of Er^{3+} :LaOF oxyfluoride borosilicate glass ceramics

Shuilin Chen, Shilong Zhao*, Fei Zheng, Chi Zhang, Lihui Huang, Shiqing Xu*

College of Materials Science and Engineering, China Jiliang University, Hangzhou 310018, China

Received 3 August 2012; received in revised form 19 September 2012; accepted 20 September 2012

Available online 28 September 2012

Abstract

Er^{3+} -doped transparent oxyfluoride borosilicate glass ceramics containing LaOF nanocrystals have been obtained by the high temperature melt-quenching and subsequent heat treatment method. The formation of LaOF nanocrystals in the glass matrix was confirmed by XRD and TEM results. In comparison with the precursor glass, Er^{3+} -doped transparent oxyfluoride glass ceramics containing LaOF nanocrystals exhibited efficient up-conversion luminescence. Especially, the green emission intensity was greatly enhanced about nearly 200 times and its up-conversion mechanism can be ascribed to a two-photon absorption process.

© 2012 Elsevier Ltd and Techna Group S.r.l. All rights reserved.

Keywords: Oxyfluoride glass ceramics; Er^{3+} ions; Up-conversion luminescence

1. Introduction

Near infrared to visible up-conversion luminescence in rare-earth (RE) doped materials has been investigated extensively owing to its potential applications such as up-conversion display, high-capacity optical data storage, optical fiber laser, etc. [1–5]. In recent years, up-conversion luminescence has re-attracted great interest due to its potential applications in improving the conversion efficiency of silicon solar cells by reducing the sub-band gap of component loss [6,7]. The up-conversion luminescence layer can be integrated at the back side of a solar cell and the first application to a silicon solar cell was reported by Shalav et al. [8]. Recently, Er^{3+} -doped NaYF_4 microprisms were applied to an amorphous silicon solar cell and 0.3 μA current was obtained under an excitation from a 980 nm laser diode (LD) [9]. However, RE ions doped fluoride phosphors are usually dispersed in an organic solvent and spin-coated at the rear side of solar cells [10]. The transmittance of the composite layer

decreases rapidly due to the scattering of fluoride phosphors [11], which is disadvantageous for the application on solar cells.

In order to obtain transparent bulk materials, RE ions doped oxyfluoride glass ceramics are another candidate and have attracted great attention since the pioneering work of Wang and Ohwaki [12]. This kind of material combines the low phonon energy of fluoride crystals and excellent mechanical and chemical performances of oxide glasses. The up-conversion efficiency of RE ions in the oxyfluoride glass ceramics depends largely on the energy level structure of RE ions and local environment [3]. Lanthanum oxyfluoride (LaOF) is an important host matrix due to its high thermal and chemical stability, superior luminescence quantum efficiency and low phonon energy [13]. It has been reported that RE doped LaOF could generate much higher emission intensity than RE doped LaF_3 [14]. However, a few reports were concentrated on the luminescence of RE doped glass ceramic containing LaOF nanocrystals [15]. In this paper, Er^{3+} :LaOF oxyfluoride borosilicate glass ceramics were prepared by the conventional melting and thermal treatment methods, and the up-conversion luminescence of Er^{3+} ions in the glass ceramics was investigated as an up-converter of amorphous silicon solar cells.

*Corresponding authors. Tel.: +86 571 8683 5781;
fax: +86 571 2888 9527.

E-mail addresses: shilong_zhao@hotmail.com (S. Zhao),
sxucjlu@hotmail.com (S. Xu).

2. Experimental

The precursor glass was prepared with molar composition of $63\text{SiO}_2\text{--}15\text{B}_2\text{O}_3\text{--}16\text{Na}_2\text{O}\text{--}5.5\text{LaF}_3\text{--}0.5\text{ErF}_3$. The mixed raw materials were melted in a covered alumina crucible at 1350°C for 40 min. The glass melt was quenched into a preheated brass mold. The quenched sample was annealed at 450°C for 2 h and then cooled slowly down to the room temperature. The differential thermal analysis (DTA) result of the precursor glass indicated that no evident crystallization peak was observed in the DTA curve. To obtain transparent oxyfluoride glass ceramics, the precursor glass was heat-treated at 615, 625, and 635°C for 2 h, and was named as GC-615, GC-625, and GC-635, respectively. X-ray diffraction (XRD) measurements were performed on Rigaku D/max2550V/PC diffractometer with Cu-K_α radiation (40 kV, 40 mA). The microstructure of GC-625 was analyzed by a transmission electron microscope (TEM, Philips-FEI-Tecnaï G2 F30) operating at an accelerating voltage of 200 kV. The sample for TEM analysis was prepared by depositing a drop of a colloidal ethanol solution of the glass-ceramic powder onto a carbon coated copper grid. The excess liquid was wicked away with filter paper, and the grids were dried in air. Up-conversion luminescence was performed with a Jobin-Yvon Frolog3 fluorescence spectrophotometer

excited by a 980 nm LD. All measurements were taken at room temperature.

3. Results and discussion

Fig. 1 shows the XRD patterns of the precursor glass and glass ceramics. The precursor glass is completely amorphous with no diffraction peaks. After crystallization, strong diffraction peaks appear and are easily assigned to trigonal LaOF (JCPDS No. 06-0281). With the increase of heat treatment temperature, the diffraction peaks become more evident and sharper, which indicates crystalline phase increases and grows gradually. When the heat treatment temperature is elevated to 635°C , another crystalline phase LaF_3 occurs. In order to control the crystallization of single phase LaOF in the glass matrix, 625°C is selected as the optimum temperature.

From the peak width of XRD pattern, the crystalline size of LaOF crystals in the glass ceramics can be estimated by using Scherrer's equation:

$$D = K\lambda / \beta \cos \theta \quad (1)$$

where D is the crystalline size at the vertical direction of (hkl) , λ is the wavelength of X-ray, θ is the angle of diffraction peak, β is the full-width at half maximum (FWHM) of the diffraction peak and the constant K is determined by β and the instrument. The diffraction peak at $2\theta = 26.96^\circ$ was used to obtain the crystalline size of LaOF crystal, and the values in GC-615, GC-625 and GC-635 were found to be about 28 nm, 33 nm and 57 nm, respectively.

Fig. 2(a) shows the TEM image of GC-625. The dark and nearly spherical particles are the precipitated LaOF nanocrystals, which distribute homogeneously among glass matrix and may be a key factor for determining the optical performance of the glass ceramic. The crystalline size is in the range of 25–35 nm, which is consistent with the calculated result based on the XRD data. The high-resolution TEM (HRTEM) image, as given in Fig. 2(b), shows the resolved lattice fringes with a constant spacing of 0.332 nm, ascribed to the $(0\ 1\ 2)$ plane of LaOF nanocrystal,

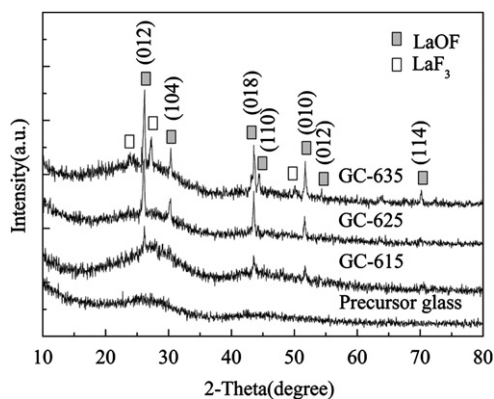


Fig. 1. XRD patterns of the precursor glass and glass ceramics.

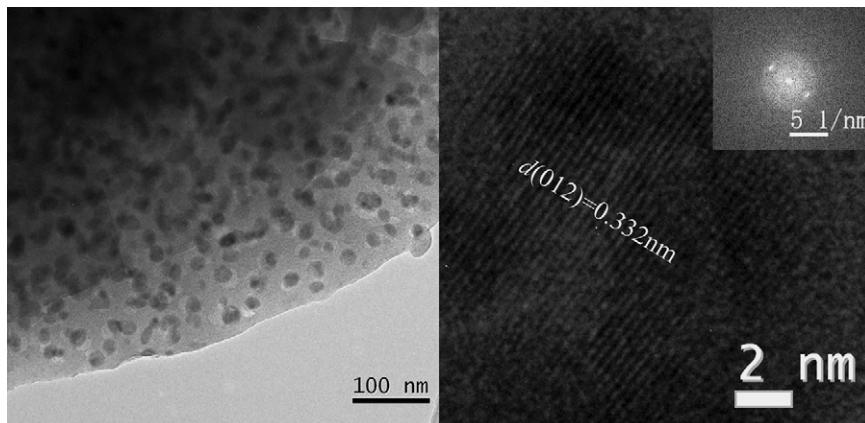


Fig. 2. TEM (a) and HRTEM (b) photograph of GC-625; inset: FFT pattern of HRTEM.

indicative of the high degree of crystallinity. The inset shows the fast Fourier transformation pattern (FFT) obtained from a selected area of HRTEM.

Fig. 3 shows the transmittance spectra of Er^{3+} -doped glass and glass ceramics. Ten absorption bands at 1535 nm, 975 nm, 800 nm, 650 nm, 540 nm, 520 nm, 487 nm, 451 nm, 408 nm and 379 nm can be assigned to the ground state $^4\text{I}_{15/2}$ to the excited states $^4\text{I}_{13/2}$, $^4\text{I}_{11/2}$, $^4\text{I}_{9/2}$, $^4\text{F}_{9/2}$, $^4\text{S}_{3/2}$, $^2\text{H}_{11/2}$, $^4\text{F}_{7/2}$, $^4\text{F}_{5/2}+^4\text{F}_{3/2}$, $^2\text{G}_{9/2}$, and $^2\text{G}_{11/2}$ transitions of Er^{3+} ions, respectively. The transmittance of glass ceramics decreases gradually with the increase of heat treatment temperature due to the crystallization processes. However, the transmittance of GC-625 around 500 nm is still nearly 80%, which is very advantageous for the application on the silicon solar cells. It is noticed that strong absorption peaks at 980 nm and 1530 nm appear, which are useless for the amorphous silicon solar cells, but they are very beneficial for improving the performance of amorphous silicon solar cells. To identify the ability of $\text{Er}^{3+}:\text{LaOF}$ glass ceramics as a

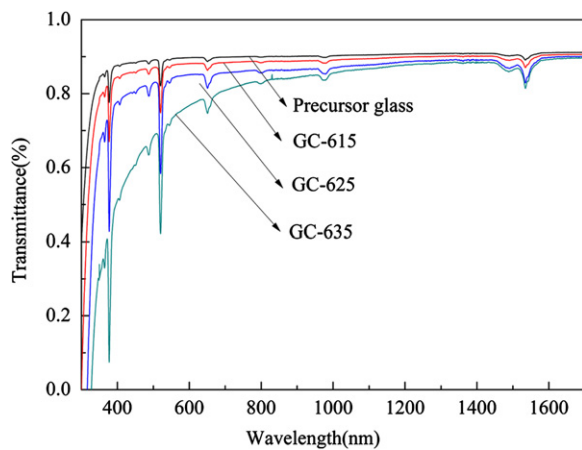


Fig. 3. Transmittance spectra of the precursor glass and glass ceramics.

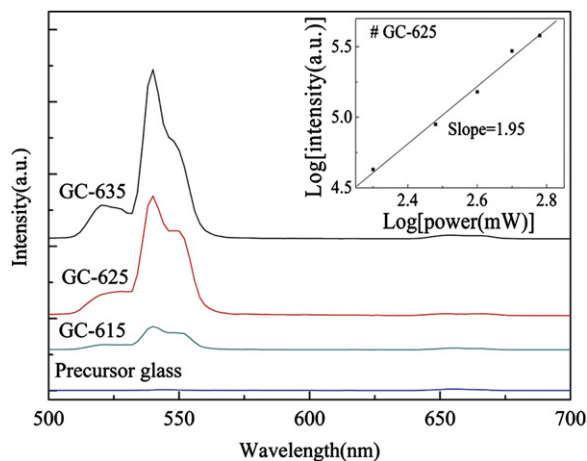


Fig. 4. Up-conversion spectra of the precursor glass and glass ceramics; inset: relationship between the up-conversion intensity of GC-625 and pumping power.

good up-converter material, the up-conversion spectra must be considered [16].

The up-conversion spectra of Er^{3+} ions in the precursor glass and glass ceramics excited at a pump power 200 mW are shown in Fig. 4. In the precursor glass, the up-conversion luminescence of Er^{3+} ions can hardly be detected. However, intense up-conversion luminescence of Er^{3+} ions can be observed after heat treatment, indicating the enhancement of up-conversion luminescence originated mainly from the Er^{3+} ions in LaOF nanocrystals. The strong green emission bands at 520 nm and 540 nm correspond to $^2\text{H}_{11/2} \rightarrow ^4\text{I}_{15/2}$ and $^4\text{S}_{3/2} \rightarrow ^4\text{I}_{15/2}$ transitions, respectively and the weak red emission bands at 655 nm is assigned to $^4\text{F}_{9/2} \rightarrow ^4\text{I}_{15/2}$ transition. It is well known that the intensity of up-conversion luminescence is very sensitive to the multi-phonon relaxation rate of RE ions. Usually, the lower the phonon energy of host matrix is, the smaller the multi-phonon relaxation probability is. The maximum phonon energy in silicate oxide glass is about 1100 cm^{-1} and that in borate oxide glass is about 1400 cm^{-1} . However, the maximum phonon energy of LaOF is 406 cm^{-1} [17], which is significantly lower than those in the precursor glasses. Thus, the variation of coordination environment around Er^{3+} ions after crystallization may result in the significant enhancement of up-conversion luminescence intensity in the glass ceramics. To investigate the required photon number involved in populating the $^2\text{H}_{11/2}$ and $^4\text{S}_{3/2}$ levels, the pumping power dependence on the up-conversion emission intensities has been determined, as shown in the inset of Fig. 4. The following relationship exists between the up-conversion emission intensity I_{em} and the IR excitation intensity I_{ex} : $I_{\text{em}} \propto (I_{\text{ex}})^n$, where n is the number of IR photons absorbed per visible photon emitted. Therefore, a plot of $\log(I_{\text{em}})$ versus $\log(I_{\text{ex}})$ should yield a straight line with the slope n . The slope is 1.95, which indicates that the up-conversion luminescence is related to two-photon absorption processes.

Fig. 5 depicts the energy level diagram of Er^{3+} ions as well as the possible up-conversion mechanisms accounting for the green and red emissions. For the green emission, firstly, Er^{3+} ion at $^4\text{I}_{15/2}$ level absorbs a 980 nm photon and is excited to $^4\text{I}_{11/2}$ level through the ground state absorption (GSA). After heat treatment, Er^{3+} ions are

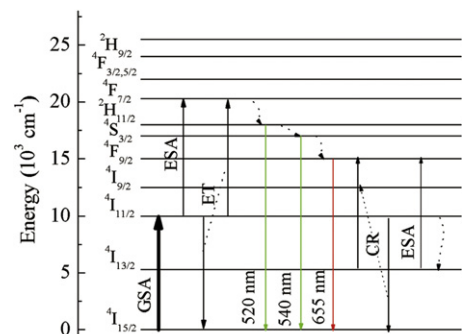


Fig. 5. Energy level diagram of Er^{3+} ions as well as the proposed up-conversion mechanism.

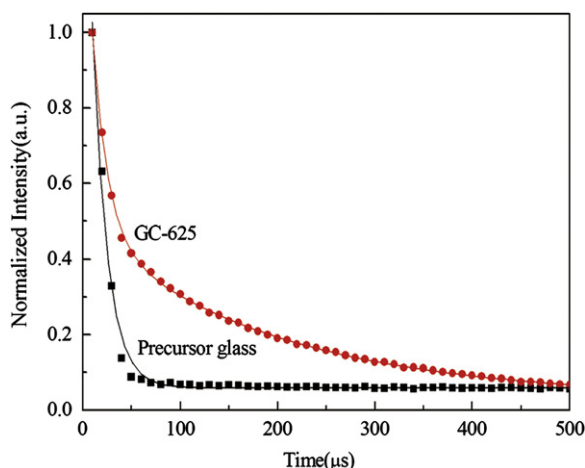


Fig. 6. Fluorescence decay curves of the $^4S_{3/2}$ level of Er^{3+} in the precursor glass and GC-625.

embedded in the precipitated LaOF nanocrystals and the energy transfer (ET) efficiency of the neighboring Er^{3+} ions increase. Thus, Er^{3+} ion at $^4I_{11/2}$ is excited further to $^4F_{7/2}$ through excited state absorption (ESA) or ET process between adjacent Er^{3+} ions. Er^{3+} ions populated at $^4F_{7/2}$ level decay non-radiatively to the next lower energy levels $^2H_{11/2}$ and $^4S_{3/2}$, and later transition to the ground state and produce 520 nm and 540 nm green emissions, respectively. The red emission at 655 nm is originated from the $^4F_{9/2} \rightarrow ^4I_{15/2}$ transition. The $^4F_{9/2}$ level of Er^{3+} ions can be populated by three possible mechanisms. The first possible mechanism is that $^4S_{3/2}$ state of Er^{3+} ions decays non-radiatively to the lower energy state $^4F_{9/2}$ through a multiphonon relaxation process. Secondly, the long living $^4I_{13/2}$ level, which is a non-radiative relaxation from the $^4I_{11/2}$ level, was excited to the $^4F_{9/2}$ level by the ESA process. Thirdly, a cross relaxation process between $^4I_{13/2}$ and $^4I_{11/2}$ also contributes to the population of the $^4F_{9/2}$ level.

Fig. 6 shows the fluorescence decay curves of $^4S_{3/2}$ level by monitoring the $^4S_{3/2} \rightarrow ^4I_{15/2}$ emission line (540 nm) for the precursor glass and GC-625 samples. The decay curve for the precursor glass can be approximately fitted by a single exponential function with a lifetime of 15.3 μs , while that for GC-625 can be fitted by a two-exponential function with one lifetime of 15.4 μs and the other of 194.5 μs , suggesting the presence of two Er^{3+} sites, i.e., one in the glass matrix (with short lifetime) and the other in the crystalline environment (with long lifetime).

4. Conclusions

New Er^{3+} -doped transparent oxyfluoride borosilicate glass ceramics containing LaOF nanocrystals have been prepared by heat treatment of $63SiO_2-15B_2O_3-16Na_2O-5.5LaF_3-0.5ErF_3$ glass. The up-conversion emission of Er^{3+} ions in the glass ceramics can be observed to be much stronger than that in the precursor glass, and the green emission of GC-625 is greatly enhanced nearly 200 times. The transition mechanism of the green emission can

be ascribed to a two-photon absorption process. The fluorescence decay curves indicated that the lifetime of $^4S_{3/2}$ state of Er^{3+} in the glass ceramic was longer than that in the precursor glass. These results indicated that Er^{3+} -doped transparent oxyfluoride glass ceramics containing LaOF nanocrystals can be used as a potential up-converter material for improving the efficiency of silicon solar cells.

Acknowledgments

This work was financially supported by the National Natural Science Foundation of China (51072190 and 11004177), the Zhejiang Provincial Natural Science Foundation of China (Y4110621 and Z4100030), and the Qianjiang Talents Project of Zhejiang Province (2010R10024).

References

- [1] F. Wang, Y. Han, C.S. Lim, Y. Lu, J. Wang, J. Xu, H. Chen, C. Zhang, M. Hong, X. Liu, Simultaneous phase and size control of upconversion nanocrystals through lanthanide doping, *Nature* 463 (2010) 1061–1065.
- [2] H.T. Wong, H.L.W. Chan, J.H. Hao, Towards pure near-infrared to near-infrared upconversion of multifunctional $GdF_3:Yb^{3+}, Tm^{3+}$ nanoparticles, *Optics Express* 18 (2010) 6123–6130.
- [3] X.P. Fan, J. Wang, X.S. Qiao, M.Q. Wang, Preparation process and upconversion luminescence of Er^{3+} doped glass ceramics containing Ba_2LaF_7 nanocrystals, *Journal of Physical Chemistry B* 10 (2006) 5950–5954.
- [4] D.Q. Chen, Y.S. Wang, Y.L. Yu, P. Huang, Intense ultraviolet upconversion luminescence from $Tm^{3+}/Yb^{3+}:\beta-YF_3$ nanocrystals embedded glass ceramic, *Applied Physics Letters* 91 (2007) 051920.
- [5] L.H. Huang, T. Yamashita, R. Jose, Y. Arai, T. Suzuki, Y. Ohishi, Intense ultraviolet emission from Tb^{3+} and Yb^{3+} codoped glass ceramic containing CaF_2 nanocrystals, *Applied Physics Letters* 90 (2007) 131116.
- [6] A. Shalav, B.S. Richards, M.A. Green, Luminescent layers for enhanced silicon solar cell performance: up-conversion, *Solar Energy Materials and Solar Cells* 91 (2007) 829–842.
- [7] A.C. Pan, C. Cañizo, E. Cánovas, N.M. Santos, J.P. Leitão, A. Luque, Enhancement of up-conversion efficiency by combining rare earth-doped phosphors with PbS quantum dots, *Solar Energy Materials and Solar Cells* 94 (2010) 1923–1926.
- [8] A. Shalav, B.S. Richards, T. Trupke, K.W. Krämer, H.U. Güdel, Application of $NaYF_4:Er^{3+}$ up-converting phosphors for enhanced near-infrared silicon solar cell response, *Applied Physics Letters* 86 (2005) 013505.
- [9] Y. Chen, W. He, Y. Jiao, H. Wang, X. Hao, J. Lu, S. Yang, $\beta-NaYF_4:Er^{3+}(10\%)$ microprisms for the enhancement of a-Si:H solar cell near-infrared responses, *Journal of Luminescence* 132 (2012) 2247–2250.
- [10] J.C. Boyer, N.J.J. Johnson, F.C.J.M. Veggel, Upconverting lanthanide-doped $NaYF_4$ -PMMA polymer composites prepared by in situ polymerization, *Chemistry of Materials* 21 (2009) 2010–2012.
- [11] R.T. Chai, H.Z. Lian, Z.Y. Hou, C.M. Zhang, C. Peng, J. Lin, Preparation and characterization of upconversion luminescent $NaYF_4:Yb^{3+}, Er^{3+} (Tm^{3+})/PMMA$ bulk transparent nanocomposites through in situ photopolymerization, *Journal of Physical Chemistry C* 114 (2010) 610–616.
- [12] Y. Wang, J. Ohwaki, New transparent vitroceramics codoped with Er^{3+} and Yb^{3+} for efficient frequency upconversion, *Applied Physics Letters* 63 (1993) 3268–3270.

- [13] N. Rakov, J.A.B. Barbosa, R.B. Guimarães, G.S. Maciel, Spectroscopic properties of Eu^{3+} - and $\text{Eu}^{3+}:\text{Yb}^{3+}$ -doped LaOF crystalline powders prepared by combustion synthesis, *Journal of Alloys and Compounds* 534 (2012) 32–36.
- [14] D.L. Gao, H.R. Zheng, Y. Yu, Y. Lei, M. Cui, E.J. He, X.S. Zhang, Spectroscopic properties of Tm^{3+} and Ln^{3+} ($\text{Ln}^{3+} = \text{Yb}^{3+}, \text{Er}^{3+}, \text{Pr}^{3+}, \text{Ho}^{3+}, \text{Eu}^{3+}$) co-doped fluoride nanocrystals, *Science in China Series G* 40 (2010) 287–295.
- [15] M. Rozanski, K. Wisniewski, J. Szatkowski, C. Koepke, M. Środa, Effect of thermal treatment on excited state spectroscopy of oxyfluoride borosilicate glass activated by Pr^{3+} ions, *Optical Materials* 31 (2009) 548–553.
- [16] F.X. Xin, S.L. Zhao, L.H. Huang, S.Q. Xu, Up-conversion luminescence of Er^{3+} -doped glass ceramics containing $\beta\text{-NaGdF}_4$ nanocrystals for silicon solar cells, *Materials Letters* 78 (2012) 75–77.
- [17] J. Hölsä, B. Piriou, M. Räsänen, IR- and Raman-active normal vibrations of rare earth oxyfluorides, REOF; RE=Y, La, and Gd, *Spectrochimica Acta Part A: Molecular Spectroscopy* 49 (1993) 465–470.